Reaction-Bonded Titanium Nitride Ceramics

A. Pivkina,[a,b] P. J. van der Put,[a]* Yu. Frolov[b] & J. Schoonman[a]

[a]Laboratory for Applied Inorganic Chemistry, Delft University of Technology, PO Box 5045, 2600 GA Delft, The Netherlands
[b]Institute of Chemical Physics, Kosygina Street 4, 117977 Moscow, Russia

Abstract

Reaction-bonded titanium nitride (RBTN) ceramics were formed using high surface area titanium powder (surface area 20 m^2 g^{-1}), and nitrogen gas as precursor reactants. The titanium precursor was made by the combustion synthesis technique.[1] Owing to their microstructure and internal porosity, the metal particles are highly reactive towards nitrogen, and can be fully converted to the mononitride at comparatively low temperatures and short reaction times. Nitridation kinetics of these powders were determined at temperatures of up to 1000°C by means of insitu gravimetry. Dry-pressed binderless porous titanium pellets were heat-treated in pure nitrogen at temperatures of up to 1000°C, and fully converted to the porous TiN compacts with dimensional changes less than 5%. A reaction mechanism is proposed. The difference between the relative density of the final product and the packing density of the green body was negligibly small, but there is a considerable increase in the gas permeability and mechanical strength during nitridation. The porous end product is a suitable matrix for further applications and for making composites by infiltration deposition.

1 Introduction

Reaction bonding is a well-established ceramic forming method.[2] Of the many conceivable ceramic materials that can be made by reaction bonding, so far only reaction-bonded silicon nitride (RBSN) and reaction-bonded silicon carbide (RBSC) are produced on a commercial scale. These reaction-bonded products have acceptable to good properties, yet are not fully dense as a result of the use of gaseous reactants. The main benefit of reaction-bonding is that it produces near net shape articles.

TiN has good intrinsic properties such as high hardness, high electronic conductivity and a low coefficient of friction, but is not a mainstream structural ceramic. Titanium nitride ceramics are difficult to process, except by chemical vapour deposition (CVD), due to low sinter activity and low diffusion rates.

The use of self-heating synthesis (SHS) of refractory materials has gained attention in recent years,[1,3] but these SHS products are not reaction-bonded ceramics. This raises the question of whether reaction bonding is feasible as a near net shape processing technique for titanium nitride ceramics. Several patents exist[4–6] on high-temperature synthesis of reaction-bonded titanium nitride (RBTN) from coarse (sponge) titanium powder using nitrogen and ammonia precursors. The low diffusion coefficients in TiN, however, slow down the reaction-bonding processes and preclude formation of RBTN other than by brute force. Surface coating of the titanium particles with TiN, which shields the interior of the particles from nitridation, prevents full conversion when reacting titanium with nitrogen to titanium mononitride. The Pilling–Bedwordth rule would predict stable scale formation and self-limitation in the titanium nitridation reaction. However, by using specially tailored Ti powders made by a new technique,[1] we have observed that full conversion of the metal to porous RBTN under mild conditions is possible, as this paper will show. The nature of the solid precursor particles, in particular their surface area, is the main limiting factor for the possibility of processing reaction-bonded ceramics based on passivating scale-forming metals.

After a short description of the combustion wave method, which is a novel way for forming the high surface area titanium precursors, this paper will concentrate on nitridation kinetics of titanium powder and green pressed compacts, and also on the morphological aspects of reaction-bonded titanium nitride. Mechanical strength and argon permeability of the compacts are reported.

*To whom correspondence should be addressed.

2 Synthesis and Characterization of Titanium Powder made by the Combustion Wave Method

The metal precursor used for RBTN was a novel type of titanium powder supplied by the Institute of Chemical Physics, Moscow. The method for making the high surface area titanium powders is based on high-temperature reduction of TiO_2 using magnesium as a reductant. Commercial grade TiO_2 paint pigment powders (99·8%) were mixed with a slight excess of fine Mg powder (99·7%, 44 μm), and pressed into cylindrical tablets (diameter 5 cm, height 20 cm, porosity 10%). They were put into a reactor under argon (1 bar), and locally heated for ignition. The heat of the SHS reaction:

$$TiO_2 + 2\,Mg \rightarrow Ti + 2\,MgO \quad (\Delta H = -330\ \text{kJ mol}^{-1})$$

is sufficient to sustain the conversion reaction once ignited. In the reaction front of the combustion wave the measured maximum temperatures were > 2000°C.

The solid product, which consists of a mixture of Ti, unreacted Mg, MgO and unreacted TiO_2, was leached with hydrochloric acid, washed with distilled water, dried, milled and sieved in air. Analysis revealed the following impurities (weight percent): 0·8% Mg; 0·5% MgO; 2% TiO_2; 0·01% Cl.

Figures 1(a) and (b) show scanning electron micrographs of the titanium powder particles. Some self-similarity is observable in these powders.

The specific surface area of the titanium powders was measured by BET using krypton. It varied with particle (cluster) size as Fig. 2 shows. The particle size fractions were 1, 15 and 200 μm. Assuming self-similarity, one obtains a surface fractal dimension of 2·67,[7] a value as high as that of porous coconut charcoal. Such a high surface dimension suggests a gas-phase mechanism rather than a liquid intermediate during reductive formation of the powder.

It is of some interest to compare the morphologies of the titanium powders obtained by different methods. The industrial Kroll method of producing sponge titanium by reducing $TiCl_4$ in molten magnesium yields metal powders having a specific surface area of the order of 0·1 m^2 g^{-1} after milling. For contrast to the morphology of the combustion wave generated titanium powder, the morphology of a commercial sample of sponge titanium powder is given in Fig. 1(c).

Since the adiabatic reaction temperature is well above the melting points of magnesium and titanium dioxide, and the reaction times are short, the SHS process for the novel titanium powders consists of a complicated set of local reactions between solid, liquid and vapour phases, leading to coral-like morphologies and high specific
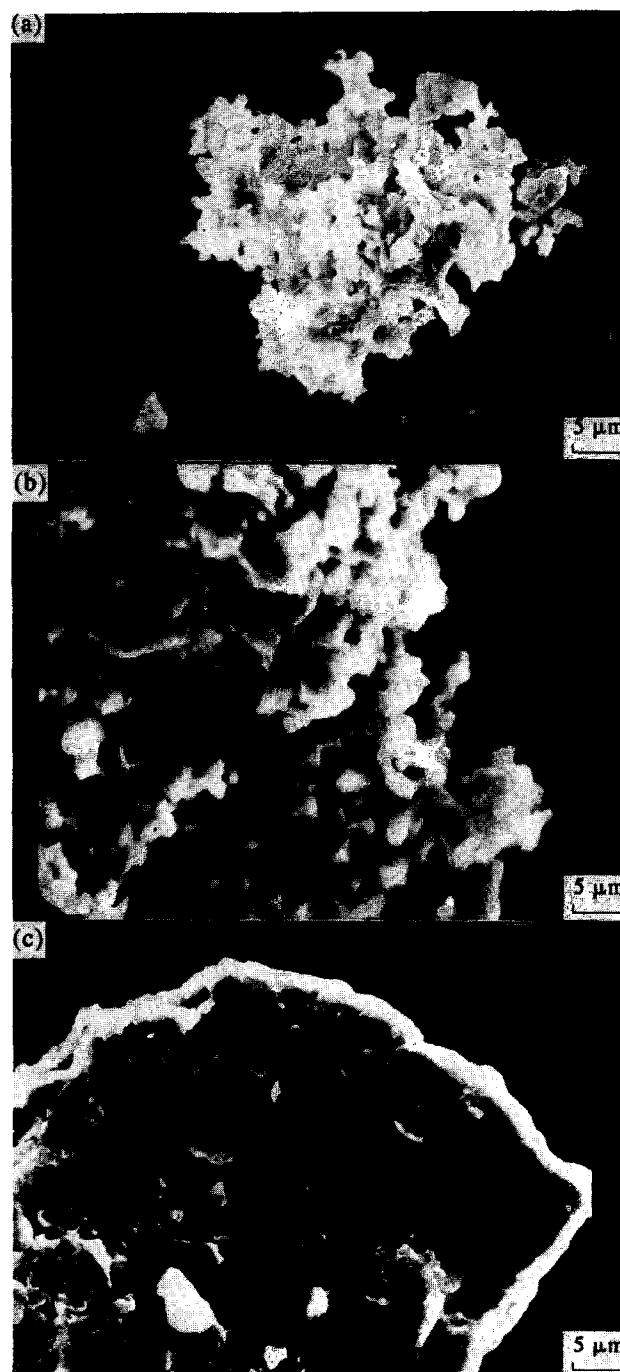

Fig. 1. SEM micrographs of combustion wave generated titanium particles: (a) d = 15 μm, (b) d = 200 μm, (c) industrial Kroll Ti particle, d = 63 μm.
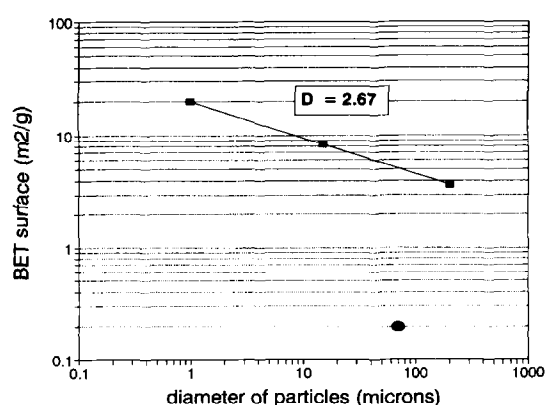

Fig. 2. Measured specific area of Ti powders as a function of particle size; ■, combustion wave generated Ti; ●, industrial Kroll Ti.

surface areas (up to 20 m² g⁻¹). The combustion wave method for making high surface area metal powders, which are stable enough for use as precursors of reaction-bonded nitride ceramics, is a convenient process which can be scaled up for bulk production.

3 Nitridation of Titanium Powder and Dry-pressed Powder Compacts to RBTN

Direct conversion of the combustion wave generated titanium precursor to TiN by reaction with pure nitrogen was studied with two groups of samples: free uncompacted loose powder, and compacted green pellets, dry-pressed from the metal powder. The nitridation rates were determined by *in situ* thermogravimetry, and the product characteristics were studied using X-ray diffraction (XRD), metallography and porosimetry.

3.1 Materials, samples and methods; experimental aspects
The nitrogen and argon gases used were supplied by Air Products and had a purity of >99·9999% and >99·9995%, respectively. The gases were further purified to a level of 5×10^{-8} of oxygen-containing species by a packed bed of titanium granules kept at a temperature of 660°C.

The particle size, surface area and morphology of the unreacted and reacted powders and compacts were characterized using scanning electron microscopy (SEM; Jeol, JSM-35), BET measurements (Micrometric Instrument Corporation), an XRD system (Philips PW 1840/01/11), and Mercury intrusion porosimetry (Porosimeter 2000).

The preparation process for the Ti pellets was as follows: precursor powder was hydraulically pressed under vacuum ($P_{max} = 3·8$ kbar). Pellets were 1 cm in diameter and about 0·05 cm thick. The porosity as measured from the external size of a weighed pellet varied between 0·20 and 0·45. The degree of homogeneity of the Ti tablets was established by optical micrographs and scanning electron microscopy. The C-ring diametral compression test was performed as previously described,[8] with Ti and TiN rings for the mechanical strength evaluation. The nitridation kinetics of titanium powders and green powder compacts were determined by *in situ* measurement of the sample weight increase in a vertical tube CVD reactor equipped with a thermobalance (C.I. Electronics Microforce Balance) with vacuum head and computer control unit. Its capacity was 5 g, the sensitivity 0·1 μg.

For the free powder nitridation experiments the platinum cup of the thermobalance was equipped
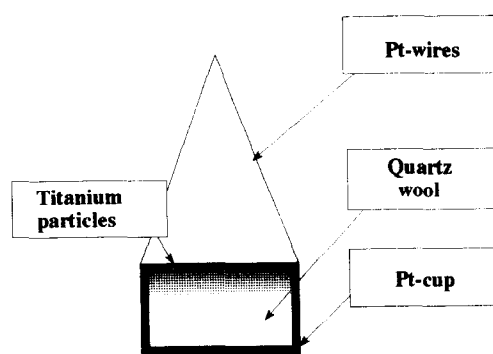

Fig. 3. Schematic presentation of the quartz wool bed used for free powder nitridation experiments.

with a quartz wool bed on which titanium powder (up to 40 mg) was placed as shown in Fig. 3. This arrangement provided uninhibited access of nitrogen to all particles. In all cases, powder having a narrow particle-size distribution was used in order to minimize the effect of packing variations.

The nitridation procedure was as follows. Initially, the samples were heated in an argon atmosphere at a rate of 100°C min⁻¹ up to the reaction temperature, which varied between 600 and 1000°C. Then the reactor was evacuated to 0·1 mbar using a single-stage mechanical rotary vacuum pump, the reactor was filled to 1 bar with nitrogen, and the weight increase recorded at constant temperature. All experiments were carried out at atmospheric pressure.

The progressive changes in the porous structure of Ti compacts before and after nitridation were evaluated using SEM observations, porosimetry and forced argon flow permeability measurements as described in Ref. 8.

3.2 Kinetics of titanium powder nitridation
As mentioned above, a thin layer of Ti particles was placed on the quartz wool bed in the platinum cup. No changes in the conversion rate were observed for samples of initial weight varying
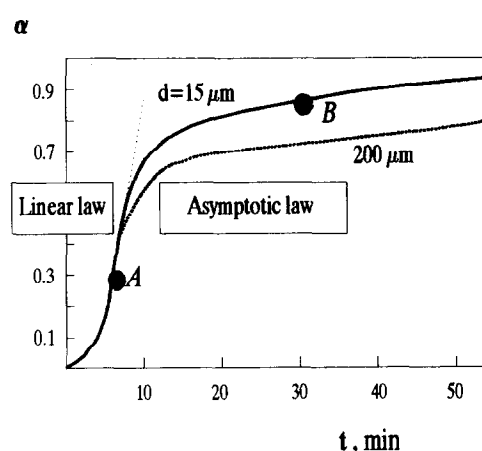

Fig. 4. Experimental nitridation kinetics of Ti particles at $T = 1000$°C. Points A and B correspond to quenched samples.

A. Pivkina et al.

from 9 to 20 mg, which indicates that there were no packing effects, and particle nitridation rates are not affected by the presence of the other particles in this weight range. Figure 4 shows the intrinsic kinetics of Ti powder nitridation as derived from the relative weight increase α measured with the thermobalance. The degree of conversion $\alpha(t)$ is defined as the instantaneous weight increase of the titanium sample during nitridation divided by the expected final weight increase on full nitridation of the titanium sample to stoichiometric TiN. After an initial transient slow rate corresponding to an incubation period due to breakdown of the passivating surface oxide film, a behaviour linear with time was observed for α at the first stage of nitridation. The relative conversion rate did not appear to depend on particle size or on the reaction temperature between 820 and 1000°C, suggesting that in the first reaction stage there is uninhibited diffusion of nitrogen into all particles, and the measured nitrogen dissolution rate is of the order of $8\cdot3 \times 10^{-4}$ mol·s^{-1}.

After attaining a degree of conversion α of approximately 0·5, the linear kinetic law changed to an asymptotic one. At this stage the conversion rate depends more strongly on temperature and particle size. As expected, higher conversion rates are observed with increasing temperature, and decreasing particle size. At comparatively modest reaction temperatures, complete conversion of titanium to titanium nitride is possible within reaction times of about 3 h. These results show that the intrinsic kinetics can be adequately described by the combination of dissolution and diffusion rate laws.

To determine reaction intermediates, some titanium powder samples were nitrided for a short time at 1000°C and subsequently quenched. The quenching procedure was as follows: the reactor was evacuated to 0·1 mbar using a mechanical rotary vacuum pump, flushed with argon to 1 bar, and cooled under argon to room temperature by removing the furnace from the fixed reactor tube. Points A and B in Fig. 4 were analyzed *ex situ* by X-ray diffraction. The presence of hcp α-Ti(N) (nitrogen-containing titanium) structures and small amounts of δ-TiN for sample A and fcc δ'-TiN as well as tetragonal δ'-TiN in sample B was established by XRD. As these phases are known to be stable on cooling to room temperature, they can be assumed to have been formed during the nitridation reaction.

These results and the phase diagram suggest the following path during reaction of titanium with nitrogen. The phase diagram for the system Ti–N has been reported by Lengauer.[9] According to the phase diagram the initial titanium particles have

the hcp structure (α-Ti), which converts to tetragonal β-Ti at a temperature of 882°C. Nitrogen dissolves in (β-Ti) up to saturation (3 at%)[10] after which threshold concentration the β-Ti lattice re-converts to the (α-Ti) hcp structure, which is able to dissolve nitrogen up to a concentration of 23 at%. Further reaction with gaseous nitrogen yields δ-TiN. According to the phase diagram tetragonal ϵ-Ti$_2$N exists at a temperature of 1000°C, but it converts to substoichiometric fcc δ-TiN.

Figure 5 represents the crystal cell volume versus nitrogen content for the Ti–N system. The titanium particles swell somewhat during nitridation as observed in SEM micrographs of sample A (Fig. 6). Increase in volume results in a decrease of the permeability of micropores inside the Ti particle, as shown by Fig. 13.

The diffusion coefficient of nitrogen in titanium solutions and titanium nitrides is reported to vary within orders of magnitude with the evolution of
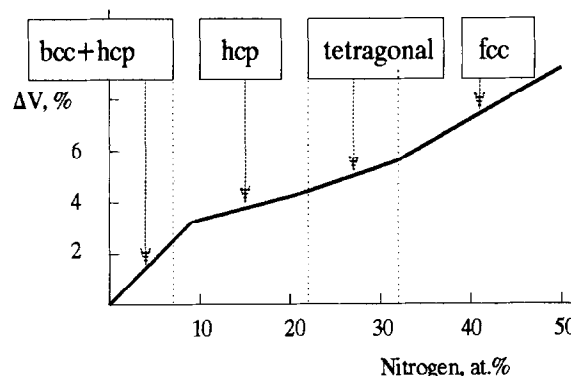
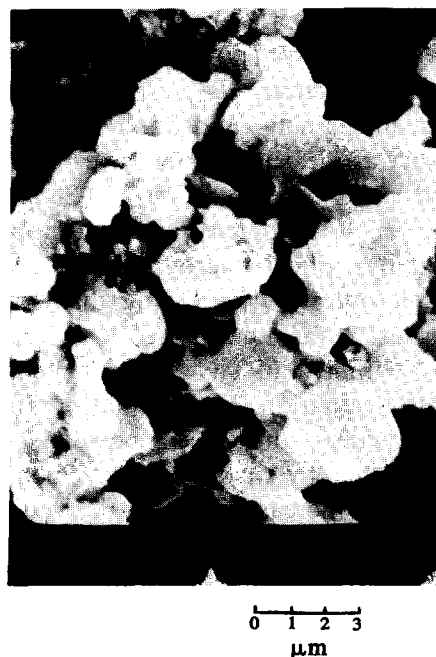Fig. 5. Predicted evolution of the crystal cell volume during Ti nitridation at 1000°C.

Fig. 6. SEM micrograph of a completely converted Ti particle. Swelling during nitridation is observed.
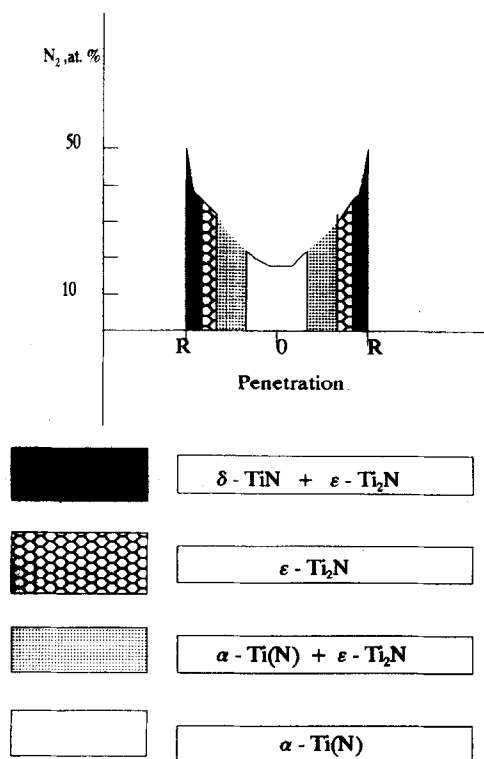
Fig. 7. Diffusion profile of nitrogen inside a Ti particle, $T = 1000°C$ (qualitative picture).

crystal structure.[10,11] The ratio of the nitrogen diffusion coefficients in β-Ti, α-Ti and δ-TiN is of the order of $100:10:1$. This suggests that titanium is first rapidly saturated with nitrogen at a rate limited by the dissolution reaction. Subsequently, nitrides form at a much slower rate which increasingly becomes diffusion limited. The observed kinetics are consistent with this reaction path. Figure 7 shows the concentration profile of nitrogen in a titanium particle during reaction. This qualitative picture, which is based on the TiN phase diagram, diffusion rates and our experimental results, reflects the evolution of the titanium particle during conversion by nitridation.

3.3 Nitridation kinetics of pressed green titanium powder compacts

Dry-pressed titanium compacts have been nitrided, and the dependence has been established of the kinetics, morphology and local degree of conversion on particle size, reaction temperature, and compact density.

Figures 8, 9 and 10 show that the overall kinetic behaviour of compacts is similar to that of free powder particles. In the initial stages of nitridation the kinetic curves of both types of sample virtually coincide. The rate of compact nitridation starts to diverge from that of powders in the asymptotic part, which is the domain of higher conversion degrees. In this much slower nitride formation step, the differences between kinetic
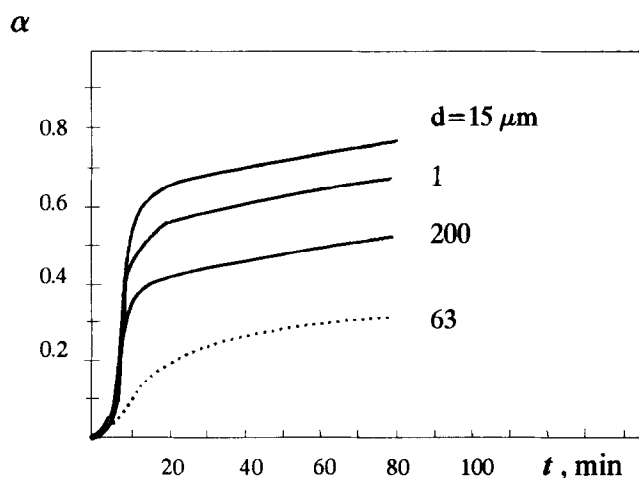

Fig. 8. Experimental nitridation kinetics of Ti pellets at 1000°C: ——, combustion wave generated Ti; ---, industrial Kroll Ti. Original particle sizes are indicated in the figure.
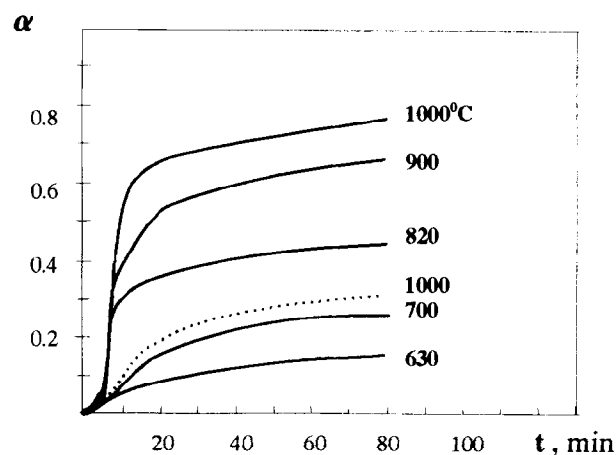

Fig. 9. Experimental nitridation kinetics of Ti pellets at different temperatures: ——, combustion wave generated Ti, original particle size 15 μm; ---, industrial Kroll Ti.
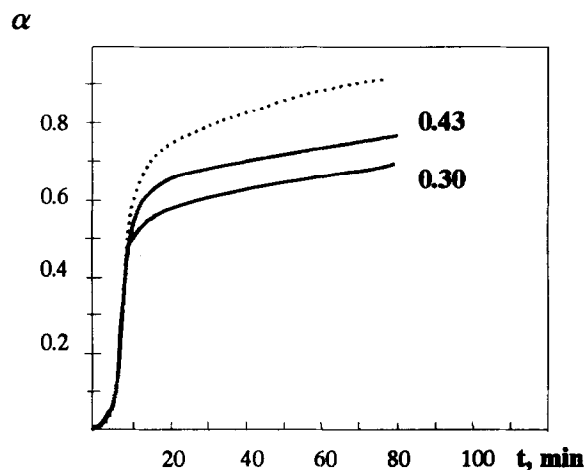

Fig. 10. Experimental nitridation kinetics of Ti pellets (——) and powder (---) at 1000°C. Values of the porosity are indicated in the figure.

behaviour of powder and compact are quite pronounced.

The titanium compacts pressed from powders having smaller primary particles reacted faster,

with the exception of powder with particle size of 1 μm. The higher surface area of the smaller particles accounts qualitatively for their enhanced reactivity in this domain. The exceptional behaviour of the 1 μm powder is probably an effect caused by the pressing process: small particles (aggregates) pack much better than the larger agglomerates when press-forged together. Therefore in the pressed compact these small particles may possibly be less accessible for the gas. Compacts made from Kroll process titanium powders were less reactive than combustion synthesized titanium, as is to be expected considering the morphology and the surface area of powders.

The reaction temperature has two effects. Higher temperatures lead to higher rates in the asymptotic domain. Second, there is no linear first stage for the pellets reacted at temperatures below 700°C. Also, this stage seems to be absent in the nitridation reaction of the Kroll titanium tablets.

Figure 10 shows the nitridation kinetics for the pellets having different porosities in comparison with intrinsic titanium powder behaviour as discussed in Section 3.2. The initial linear part of the process coincides for both types of samples, as does the conversion degree (about 25 at% of N) which separates the linear and asymptotic domains. The higher the porosity, the faster the overall reaction rate.

The microstructure of the sample which was nitrided for 3 min is shown in Fig. 11. It clearly shows the yellow-gold coloured surfaces of the grains (white in Fig. 11), as well as those of the tubular pores inside the grains. Nitrogen flow takes place through intergrain voids and the pores of individual particles (agglomerates). Particle swelling on dissolution of nitrogen is observed in SEM micrographs of this sample (Fig. 12).

Figure 13 presents the microstructure of another partially converted sample (degree of conversion: 0·73) as observed by optical microscopy; gold-

Fig. 12. SEM micrograph of the sample of Fig. 11. Particle swelling inside a porous pellet is observed.

Fig. 13. Micrograph of the cross-section of a Ti particle inside a pellet (conversion 73%).

coloured TiN crystals surround large particles which are not fully converted. The crystal structure of these particles is of interest. The dark grey and light grey parts of the titanium particles (interferometric contrast enhancement) can be attributed to two kinds of crystal structure: hcp α-Ti(N) and fcc δ-TiN$_{1-x}$. Externally, the metal particles are covered with a layer of yellow-gold TiN.

4 Microstructure and Properties of TiN Compacts

The measured difference in apparent porosity of compacts before and after nitridation was < 2%, and is within the error of experiments.

Qualitative SEM micrographs of the porous structures of untreated and nitridated samples (Figs 14(a) and (b)) indicate the structural evolution during the conversion process: the TiN compact is expected to have a larger pore size, less porous surface area and a more interconnected solid-phase network.

Heat treatment in nitrogen results in neck formation between touching particles via reaction sintering and eliminates the void phase inside the
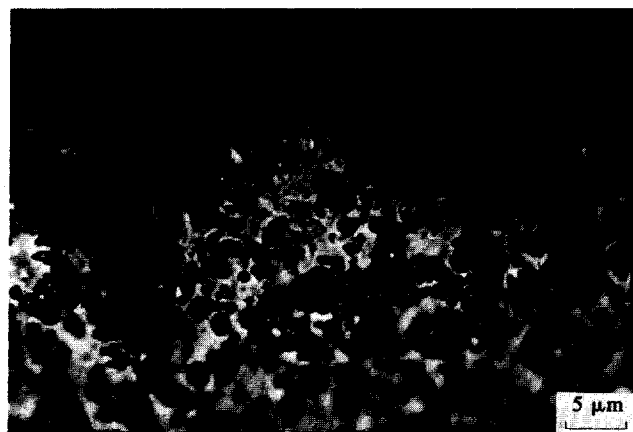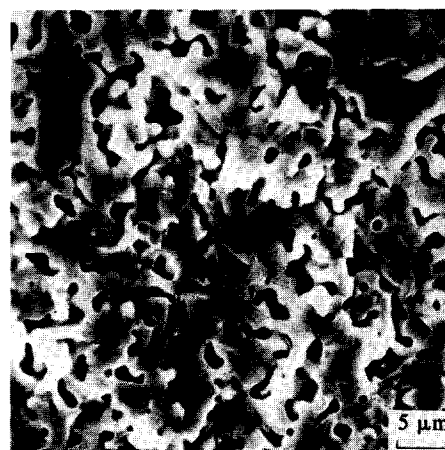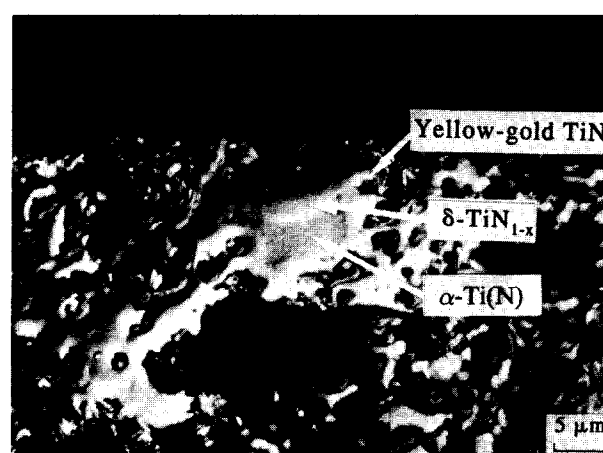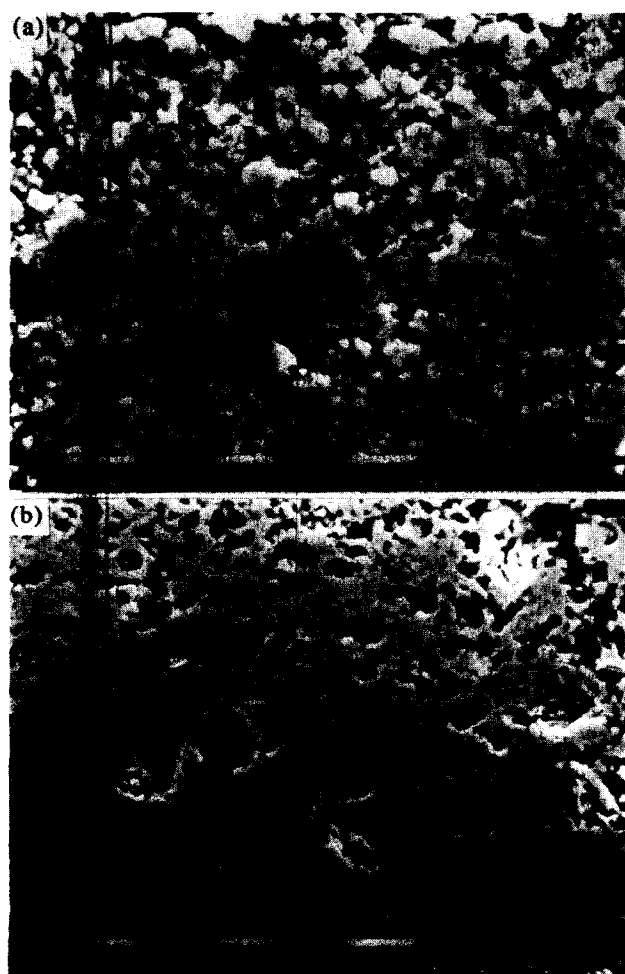

Fig. 11. Micrograph of the cross-section of a Ti pellet (nitridation time 3 min). Tubular pores in the interior of the particles and the yellow-gold surfaces of grains are observed.

Fig. 14. SEM micrographs of the compacts before (a) and after (b) nitridation.

Fig. 15. Gas permeability of two compacts labelled a and b, before and after nitridation (——, Ti; - - -, TiN).
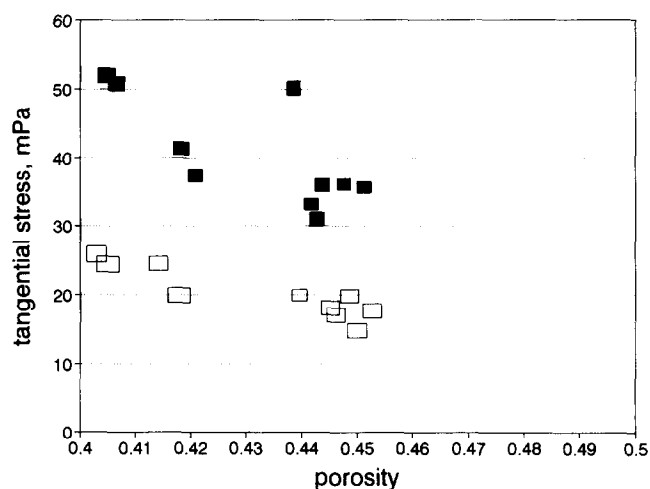
Fig. 16. Results of the C-ring diametral compression test of Ti (□) and TiN (■).

particles (or agglomerates). The titanium nitride layer formation prevents further metal matrix shrinkage, and there are slight dimensional changes of the Ti compact during nitridation, while without a nitrogen atmosphere (in argon) the Ti compact shrinks dramatically (the porosity falls from 45% to 10%) at the same temperature – time conditions.

Table 1 presents the results of mercury intrusion porosimetry. Evolution of the porous structure leads to an increase of the average pore size of up to 40%. The total surface area of the pores and interparticle voids decrease, and so does the interconnected porosity.

Results of the measurements of macroscopic properties which are strongly influenced by the pore structure, such as gas permeability and
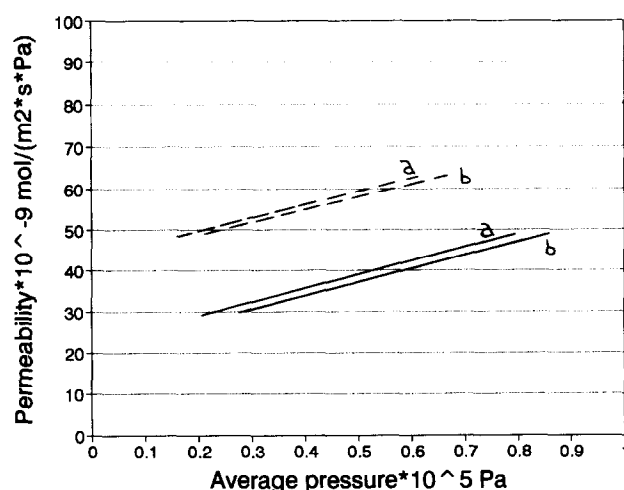
mechanical strength, are shown in Figs 15 and 16, respectively. The observed gas permeability increase up to 45% can be attributed to the growth of the pore size and the number of open pores. The strength of the compact increases considerably with nitridation, and the maximal tangential stress in Ti samples can be doubled by the present reaction-bonding process.

5 Conclusions

Porous titanium nitride ceramics can be fabricated in near net shape using combustion wave generated

Table 1. Parameters of the porous structure of compacts

		Mercury intrusion porosimetry			
	Apparent porosity	*Interconnected porosity*	*Closed porosity (%)*	*Pore radius (nm)*	*Surface of pores $(m^2 g^{-1})$*
Ti	0·443	0·392	11·5	299	2·15
TiN	0·445	0·417	6·2	422	0·91

Ti powder having a high specific surface area and a high chemical activity. The observed kinetics indicate a two-step process: a rapid dissolution of nitrogen in α-Ti, and a slower heterogeneous reaction of the nitrogen-saturated α-Ti with N_2 to TiN.

Porous Ti pellets can be fully converted to the TiN compacts with small dimensional change, and practically without a change in porosity. Also, the final product shows a considerable increase in gas permeability and mechanical strength.

These ceramics can be applied in membrane technology, as porous electrodes, and are considered to be a suitable matrix for further gas-phase infiltration treatment to form composite ceramics.

References

1. Merzhanov, A. G., *Combustion and Plasma Synthesis of High-Temperature Materials*, eds Z. A. Munir and J. B. Holt. VCH, New York, 1990, pp. 1-53.

2. Riley, F.L., Silicon nitridation. In NATO ASI Ser. E, Vol. 65, *Progress in Nitrogen Ceramics*, ed. F. L. Riley. Martinus Nijhoff Publ, Boston, 1983, p. 121.

3. Wang, L. L., Munir, Z. A. & Maximov, Y. M., Thermite reactions: their utilization in the synthesis and processing of materials. *J. Mater. Sci.*, **28** (1993) 3693-708.

4. Nakamura, Y. & Uchino, K., Titanium nitride. Japanese Patent 61 97,111 [86 97,111], 15 May 1986.

5. Nakamura, Y. & Uchino, K., Metal nitrides. Japanese Patent 61 83,604 [86 83,604], 28 April 1986.

6. Ananjin, V. N. & Belyaev, V. V., Manufacture of tubular filter from sintered Ti. *Zh. Otkrytiya i Izobreteniya*, **31** (1991) 383.

7. Avnir, D., Farin, D. & Pfeifer, P., *J. Coll. Interf. Sci.*, **103** (1985) 1112.

8. Dekker, J. P., CVD techniques for the synthesis or modification of porous ceramics. PhD thesis, Delft University of Technology, Delft, 1994.

9. Lengauer, W., The titanium–nitrogen system: a study of phase reactions in the subnitride region by means of diffusion couples. *Acta. Metall. Mater.*, **39** (1991) 2985-96.

10. Bars, J.-P., Etchessahar, E. & Debuigne, J., Etude cinétique, diffusionnelle et morphologique de la nitruration du titane par l'azote. *J. Less-Common Metals*, **52** (1976) 51-76.

11. Levinskii, Yu., Investigation of the diffusion of nitrogen in titanium. *Neorganicheskie Materialy*, **4** (1968) 2068-73.